



# Revisiting the effect of relative density on cyclic liquefaction of clean and silty sands: the crossing effect

Mehmet Murat Monkul<sup>1,2</sup> · Yunus Emre Tütüncü<sup>2</sup>

Received: 13 October 2023 / Accepted: 26 March 2024  
© The Author(s) 2024

## Abstract

Liquefaction of clean and silty sands remains to be an important problem during earthquakes. Even though many factors are known to influence liquefaction behavior, the influence of density index parameter and fines content (FC) are among the most important parameters. In this study, the effect of relative density ( $D_r$ ) on liquefaction behavior of clean and silty sands was investigated by cyclic direct simple shear tests on two different silty sands at various FC. Several different relationships affected from  $D_r$  are revisited or investigated including number of cycles to liquefaction ( $N_L$ ) and cyclic resistance ratio (CRR). It was found that liquefaction resistance-fines content-relative density relationship is much more complex than previously thought. This is because CRR- $D_r$  lines of clean and/or silty sands may cross each other at specific relative densities, which may cause the liquefaction resistance of a clean sand to be either smaller, equal or greater than the liquefaction resistance of a silty sand with the same base sand dependent on the magnitude of relative density. The mentioned behavior is also confirmed on different clean and silty sands tested in literature.

**Keywords** Liquefaction · Relative density · Fines content · Cyclic resistance ratio · Sand · Silt · Cyclic direct simple shear test

## 1 Introduction

Assessing the liquefaction potential of clean and silty sands is still one of important research topics closely related with geotechnical earthquake engineering practice. Case histories from past earthquakes have shown that both clean and silty sands could be highly liquefiable depending on the conditions (Stewart et al. 2001; Bray et al. 2004; Bhattacharya et al. 2011; Lade and Yamamuro 2011; Maurer et al. 2015; Ozener et al. 2024). Meanwhile,

---

✉ Mehmet Murat Monkul  
monkulm@oregonstate.edu

Yunus Emre Tütüncü  
emre.tutuncu@yeditepe.edu.tr

<sup>1</sup> Present Address: Courtesy Faculty, Department of Civil and Construction Engineering, Oregon State University, Corvallis, OR 97331, USA

<sup>2</sup> Department of Civil Engineering, Yeditepe University, Istanbul, Turkey

research over the past 30 years revealed that clean sands and silty sands do not show the same liquefaction resistance under similar conditions in the laboratory. Hence, influence of fines content (FC) on liquefaction resistance of sands has been intensely investigated in the last few decades, especially to figure out whether FC makes a positive or negative effect on the liquefaction resistance (Vaid 1994; Erten and Maher 1995; Xenaki and Athanasopoulos 2003; Papadopoulou and Tika 2008; Boominathan et al. 2010; Cubrinovski et al. 2010; Dash et al. 2010; Oka et al. 2018). It is also known that laboratory based research has conflicting conclusions on the subject. For instance many studies mentioned a steady drop in liquefaction resistance of sands with increasing FC until a transition or limit fines content ( $FC_L$ ) typically in between 15 and 35% (Troncoso and Verdugo 1985; Vaid 1994; Erten and Maher 1995; Xenaki and Athanasopoulos 2003; Papadopoulou and Tika 2008; Boominathan et al. 2010; Cubrinovski et al. 2010; Porcino and Diano 2017; Oka et al. 2018). Some other studies had experimental results which infer that liquefaction resistance initially increases up to a small fine content (btwn. 5%–9%); then relatively decreases (i.e. shows an initial peak) (Polito and Martin 2001; Carraro et al. 2003; Monkul et al. 2021). While another group of studies reported a steady increase in liquefaction resistance with increasing fines content (Shen et al. 1977; Amini and Qi 2000; Hazirbaba and Rathje 2009). Several other studies investigated the liquefaction behavior of clean versus silty sands based on the critical state framework, the results of which has shown that the location and slope of the critical state line are indeed affected by FC, which in turn influence their liquefaction behavior (Been and Jefferies 1985; Papadopoulou and Tika 2008; Dash et al. 2010; Stamatopoulos 2010; Wei and Yang 2019).

It should be noted that due to their complex behavior, there are countless number of experimental studies in literature investigating the undrained behavior of sand-silt mixtures from different aspects. These different aspects include but not limited to the relationship between shear wave velocity, small strain stiffness, stress anisotropy and the micro fabric of sands and sand-silt mixtures (Wichtmann and Triantafyllidis 2009; Choo and Burns 2015; Yang and Liu 2016; Payan et al. 2016, 2017; Goudarzy et al. 2016a, b, 2017, 2018; Payan and Senetakis 2019; Payan and Chenari 2019; Khodkari et al. 2024). In several of those studies, the importance of equivalent granular void ratio ( $e^*$ ), an alternative density index parameter initially proposed by Thevanayagam et al. (2002), was emphasized. In fact, the parameter of equivalent granular void ratio ( $e^*$ ) has become increasingly popular especially within the research community due its versatile capacity to capture the silty sand behavior (Rahman et al. 2008, 2012). There is no doubt that the grain characteristics including the size and shape factors also had a significant influence on the packing tendency (Sarkar et al. 2019, 2020) and resulting undrained behavior of silty sands (Monkul and Yamamuro 2011; Monkul et al. 2016). It should be reminded that density parameters other than relative density such as intergranular void ratio (Thevanayagam 1998), equivalent granular void ratio, quasi natural void ratio (Lade and Yamamuro 1997), etc. and small strain behavior of sand-silt mixtures are beyond the scope of this study, as this study focuses on the relationship between  $D_r$  and large strain behavior (i.e. cyclic liquefaction) of clean and silty sands.

Plasticity of fines (if there is any) is another aspect making the undrained behavior of silty/clayey sands even more complicated. Previous research revealed that plastic fines within a sand could also decrease its liquefaction resistance in a surprising manner. Park and Kim (2013) reported that cyclic liquefaction resistance of sands with plastic fines could decrease with an increase in the plasticity index (PI) of the fines in the sand, especially at dense states. Eseller-Bayat et al. (2019) demonstrated that different factors including FC, PI of the fines, magnitude of cyclic loading (i.e. CSR) and relative density have indeed coupled effects on cyclic liquefaction resistance of sands. For instance, under low

CSR values (i.e.  $\leq 0.1$ ) and medium dense states ( $D_r \sim 50\%$ ), sand with 10% highly plastic fines was shown to have notably less liquefaction resistance than the same base sand with 10% non-plastic fines. In fact, the observations and findings of both Park and Kim (2013) and Eseller-Bayat et al. (2019) support each other and imply that plasticity of fines within a sand might not always be a positive merit for cyclic liquefaction resistance of silty/clayey sands. Regarding the monotonic undrained response, Papadopoulou and Tika (2016) concluded that there is a threshold plasticity index value until which the sands show more contractive tendency with increasing plasticity of the fines, once the threshold PI was exceeded, their contractive tendency decreased. The study of Goudarzy et al. (2022) also involves supporting results, in which for the specimens tested at the same clay content and  $D_r$ , sand-kaolin mixtures has shown smaller undrained shear strength (more contractive tendency) compared to the sand-bentonite mixtures.

Nevertheless, one of the reasons behind the mentioned conflicting conclusions in literature on fines content effect is the density parameter employed for comparing the liquefaction behaviors, such as void ratio ( $e$ ), intergranular void ratio ( $e_s$ ), relative density ( $D_r$ ), dry density ( $\rho_d$ ), quasi-natural void ratio etc. (Monkul et al. 2016). All of the mentioned density parameters are indeed authentic, and previous literature using different density parameters are all valuable. Therefore, the goal of this study is not to debate on the superiority of a single parameter, but rather focus on the effect of  $D_r$ . Relative density is among the most commonly used density index parameters in geotechnical earthquake engineering practice and research. Consequently, many correlations were also proposed which link relative density with popular in-situ tests such as CPT (Cone Penetration Test) tip resistance ( $q_c$ ) (Lunne et al. 1997; Jamiolkowski et al. 2001; Mayne 2007; Idriss and Boulanger 2008; Ecemis and Karaman 2014; Ghali et al. 2019) and SPT (Standard Penetration Test) blow count number ( $N$ ) (Meyerhof 1957; Whitman 1971; Tokimatsu and Yoshimi 1983; Skempton 1986; Cubrinovski and Ishihara 1999; Idriss and Boulanger 2008; Cubrinovski et al. 2010). Cubrinovski et al. (2010) stated that SPT  $N$  is more sensitive to  $D_r$  changes compared to the CPT tip resistance, which reminds the importance of relative density on in-situ test results. Even the post-liquefaction stress-strain behaviour of sands was shown to be dependent on their pre-liquefaction relative density (Rouholamin et al. 2017). Relative density is also known to influence the static shear stress correction factor ( $K_\alpha$ ) which could be especially important in the liquefaction analyses of slopes and embankments. According to the previous laboratory-based research, the value of  $K_\alpha$  might increase with increasing static shear stress ratio for soils at medium dense to dense states, indicating a greater cyclic strength. While the trend may be reversed for soils at loose states (Idriss and Boulanger 2008).

Even though  $D_r$  is a very important parameter known to influence the engineering behavior and cyclic strength of clean and silty sands, it is interesting to observe that the results of laboratory studies on liquefaction are still confusing even when  $D_r$  is selected as the comparison basis for the clean and silty sands (i.e. when they are compared at the same  $D_r$ ). For instance, some studies reported that at the same relative density, liquefaction resistance or dilatancy of silty sands are greater than that of the clean sands (Amini and Qi 2000; Salgado et al. 2000; Hazirbaba and Rathje 2009). Meanwhile, there are other studies according to which the liquefaction resistance of silty sands is smaller than that of the clean sands at the identical  $D_r$  values (Singh 1996; Boominathan et al. 2010; Cubrinovski et al. 2010; Oka et al. 2018).

Moreover, experimental results of different studies imply conflicting trends about the variation of liquefaction resistance with FC when compared at the same  $D_r$ . Cyclic triaxial tests on Ottawa sand performed by Carraro et al. (2003) and cyclic direct simple shear tests

on Silica sand performed by Monkul et al. (2021) have both shown that liquefaction resistance of sands initially increases until a minor amount of FC (e.g. 5%) then declines with further rise in silt content (below  $FC_{\downarrow}$ ) when compared at the same  $D_r$ . In fact, cyclic triaxial tests conducted by Polito and Martin (2001) on Yatesville sand have shown a similar trend at  $D_r=30\%$  (i.e. liquefaction resistance shows a peak at small FC). Kokusho (2007) run cyclic triaxial tests on three river sands adjusted to have different gradations with different FC (involving low plastic silt,  $PI=6$ ). In the same study, it was emphasized that sands' liquefaction resistance is largely dependent on  $D_r$ , however not so much sensitive to gradation and uniformity coefficient (CU). Results of Kokusho (2007) at three different relative densities (i.e.  $D_r=30\%$ ,  $50\%$  and  $70\%$ ) also revealed that liquefaction resistance of river sands tested at loose state (i.e.  $D_r=30\%$ ) have shown insignificant difference with increasing FC. However, at medium dense and dense states (i.e.  $D_r=50\%$  and  $70\%$ ), liquefaction resistance has decreased with increasing FC (below  $FC_{\downarrow}$ ). Karim and Alam (2014) run cyclic triaxial tests at constant relative density ( $D_r=60\%$ ) on fine sand-nonplastic silt mixtures from a bridge site at Bangladesh and observed that liquefaction resistance of sand has decreased with increasing fines content until  $FC_{\downarrow}$ , then remained constant afterwards.

Consequently, four different trends about the change of liquefaction resistance of sands with increasing fines content (below the  $FC_{\downarrow}$ ) were observed/reported in previous experimental studies when specimens are compared at a constant relative density value: (1) liquefaction resistance initially increases until a minor FC then relatively declines (Polito and Martin 2001; Carraro et al. 2003; Monkul et al. 2021), (2) liquefaction resistance remains almost constant with FC (Kokusho 2007), (3) liquefaction resistance decreases with FC (Singh 1996; Kokusho 2007; Boominathan et al. 2010; Karim and Alam 2014; Oka et al. 2018; Chen et al. 2020), (4) liquefaction resistance increases with FC (Amini and Qi 2000; Hazirbaba and Rathje 2009; Jradi et al. 2020). It is obvious that at a given relative density, how the fines content influences the liquefaction resistance of sands is still unclear. Is it possible that all of the mentioned trends in literature could indeed be valid? If this is true, the influence of relative density on liquefaction behavior of sands having different FC is indeed much more complicated than previously expressed in literature. This experimental study seeks an answer to this question. Constant volume cyclic direct simple shear (CDSS) tests were performed on two different silty sands at a wide range of relative density values. Testing at a relatively wide range of  $D_r$  compared to the majority of the previous studies (which mostly considered one or two  $D_r$  values) allowed authors to make deeper and more detailed observations regarding the influence of relative density on liquefaction of clean and silty sands.

## 2 Soils tested

Two different non-plastic silts (YET silt and SI silt) and two clean base sands (Silica Sand and Sile Sand 20/30) were used in the experimental program. YET silt is obtained from Kırklareli, Turkey. After it was transported to the laboratory, wet sieving was done and only the fine fraction passing No 200 sieve ( $<0.075$  mm) was used in the experiments. SI silt was also attained from Kırklareli, Turkey and was already processed in the quarry to have fines only (i.e.  $<0.075$  mm). Both YET and SI silts are found to be non-plastic, and their grain size distributions based on hydrometer tests are plotted in Fig. 1. Silica Sand and Sile Sand 20/30 were brought to the laboratory to be used as clean base

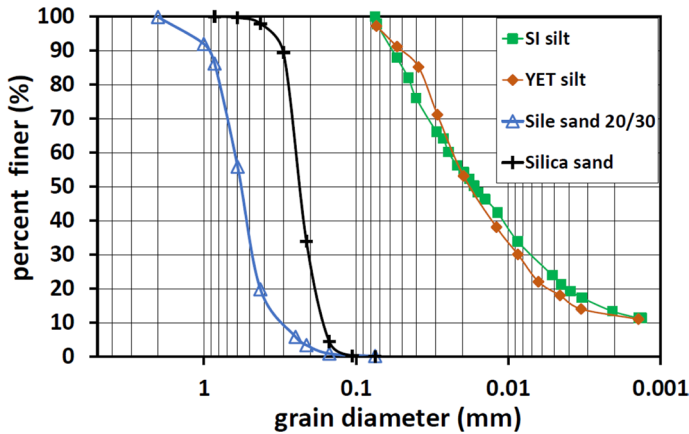
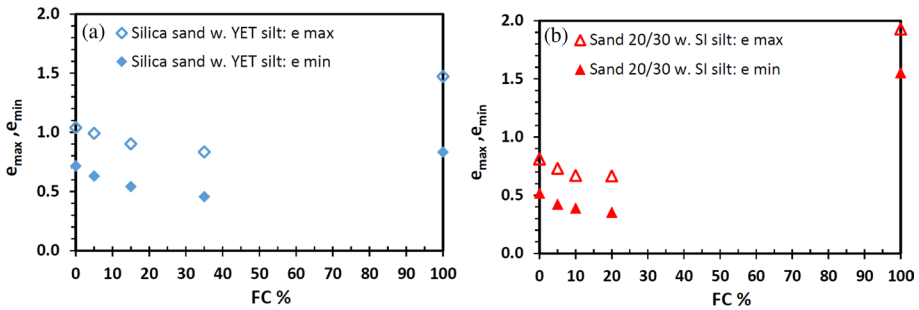


Fig. 1 Grain size distribution of the clean base sands and non-plastic silts used in the experimental program

sands from İzmir and İstanbul, Turkey respectively. Their grain size distributions were also shown in Fig. 1.

Silica sand was thoroughly mixed with YET silt, while Sile Sand 20/30 was mixed with SI silt at various fractions on dry weight basis such that the silty sands obtained would have fines contents (FC) between 0 and 35%. Soils from multiple regions were combined (mixed) in order to control the FC of resulting silty sands precisely over a relatively wide range of fines content. Moreover, both the gradations and plasticity of base sand and silt fractions are also kept the same in this way. Fines content (FC) corresponds to the proportion of soil particles in total dry weight smaller than 0.075 mm within silty sands. The fines content range studied in the present research ( $0 \leq FC \leq 35\%$ ) is expected to be within the sand dominated region based on the limiting fines content ( $FC_L$ ) values commonly declared in literature (Polito and Martin 2001; Monkul and Ozden 2007; Zuo and Baudet 2015; Monkul et al. 2017).

In order to calculate the relative density of different specimens, minimum ( $e_{min}$ ) and maximum ( $e_{max}$ ) void ratios for each silty sand were determined by the method proposed by Lade et al. (1998). This method employs a calibrated 2000 mL glass cylinder, and experimental procedure and its accuracy were explained in detail by Lade et al. (1998) for several different clean and silty sands. Note that many standards for  $e_{min}$  and  $e_{max}$  determination were conventionally intended for sands up to a limited FC value (e.g. Japanese procedure  $\leq 5\%$ , ASTM procedure  $\leq 15\%$ ) (Cubrinovski and Ishihara 2002). Because the amount of fines used in this study ( $\leq 35\%$ ) are greater than the amounts recommended by ASTM ( $\leq 15\%$ ) or Japanese ( $\leq 5\%$ ) procedures, Lade's method was used. Note that the method recommended by Lade et al. (1998) also uses the conventional definition of relative density (does not propose/define a modified  $D_r$ ) and the mentioned method was effectively implemented for obtaining the  $e_{min}$  and  $e_{max}$  for various silty sands in liquefaction research over a wide FC range (Lade and Yamamuro 1997; Yamamuro and Covert 2001; Lade et al. 2009; Monkul and Yamamuro 2011; Monkul et al. 2017, 2021). Variations of determined  $e_{min}$  and  $e_{max}$  values of sands with fines content were shown in Fig. 2a for Silica Sand and in Fig. 2b for Sile Sand 20/30. Specific gravities ( $G_s$ ) of base sands were found to be 2.64 and 2.65 for Silica Sand and Sile Sand 20/30, respectively. While  $G_s$  values for the non-plastic silts were determined as 2.64



**Fig. 2** Variation in the maximum ( $e_{max}$ ) and minimum ( $e_{min}$ ) void ratios silty sands with fines content (FC): **a** Silica sand with YET silt, **b** Sand 20/30 with SI silt

and 2.68 for YET silt and SI silt, respectively. The basic properties of the tested soils are given in Table 1.

### 3 Experimental program

All of the experimental program was done at Yeditepe University's Soil Mechanics Laboratory.

#### 3.1 Specimen preparation

Specimens of clean and silty sands were reconstituted employing the automatic dry funnel deposition technique in a cylindrical split mold adjusted to the CDSS test apparatus. Detailed explanations about the mentioned method (automatic dry funnel deposition) including the funnel raising speed, raising motor controlled by the computer, specially designed aluminum funnel, etc. are available in Monkul et al. (2018) and Monkul and Yenigun (2021). Diameter of the specimens was 64 mm, while their typical height was about 20 mm. Previous research revealed that sand and silt fractions are remained reasonably uniform with dry funnel deposition, which eliminates the segregation problem during reconstitution process for silty sand specimens (Bahadori et al. 2008; Yamamuro et al. 2008; Eseller-Bayat et al. 2019).

**Table 1** Basic properties of the tested soils

	Silica sand	Silt sand	YET silt	SI silt
$G_s$	2.64	2.65	2.64	2.68
$D_{10}$	0.165	0.310	0.001	0.001
$D_{30}$	0.205	0.465	0.009	0.012
$D_{60}$	0.247	0.630	0.024	0.025
$C_u$	1.50	2.03	16.8	18.8
$C_c$	1.03	1.11	2.30	3.97
USCS symbol	SP	SP	ML	ML

### 3.2 Cyclic direct simple shear (CDSS) tests

Constant volume stress controlled CDSS tests were done on the mentioned soils in Sect. 2. Lateral confinement was attained by Teflon-coated rings stacked around the latex membrane. After reconstitution, all specimens were consolidated to 100 kPa vertical effective stress ( $\sigma'_{vc} = 100$  kPa). After the consolidation stage, uniform sinusoidal cyclic shear stresses ( $\tau_{cy}$ ) were implemented at a rate of 0.1 Hz, which correspond to various cyclic stress ratio values (i.e.  $CSR = \tau_{cy} / \sigma'_{vc}$ ) between 0.08 and 0.14.

The constant volume condition is created by maintaining the consolidated height of specimens constant during cyclic shearing stage via computer control. More explicitly, during cyclic loading the value of vertical stress is either increased or decreased ( $\Delta\sigma_v$ ) by the computer to keep the specimens' volume constant. This change in vertical stress is known to be equal to the excess pore water pressure ( $\Delta u_e$ ) in a truly undrained test where constant volume is maintained by preventing the drainage of pore water during loading (e.g.  $+\Delta u_e = -\Delta\sigma_v$ ) (Dyvik et al. 1987; Vaid and Sivathayalan 1996; Porcino et al. 2008; Monkul et al. 2015; Li et al. 2016; Polito 2017). Similarly, it is demonstrated in literature that dry and saturated cohesionless soils (e.g. clean sands, sands with non-plastic silts) give similar cyclic response (Finn and Vaid 1977; Wijewickreme et al. 2005; Monkul et al. 2015; Viana Da Fonseca et al. 2015), hence CDSS specimens are tested in dry state during the present research.

Clean and silty sand specimens were tested at a wide range of relative density values and the total number of constant volume CDSS tests conducted in this study is 175. Among those, 85 CDSS tests were done on Silica Sand-YET silt mixtures, while remaining 90 tests were performed on Sile Sand 20/30-SI silt mixtures. Cyclic loading continued either until 10% D.A. shear strain or excess pore pressure ratio value of 1 (i.e.  $R_u = \Delta u_e / \sigma'_{vc} = 1$ ) was reached. The 10% D.A. strain might seem greater than the typical strain-based liquefaction triggering criterion of 3.75% S.A. (or 7.5% D.A.) considered for many CDSS tests in literature, e.g. (Wijewickreme et al. 2005; Porcino et al. 2008; Viana Da Fonseca et al. 2015). However, 10% D.A. is intentionally employed in the present study in order to make the difference between the two alternative liquefaction criteria (10% D.A. strain and  $R_u = 1$ ) insignificant. This can be better observed in Fig. 3 as an example output for one of the tested silty sand specimens (i.e. FC = 5%,  $D_r = 41.9\%$ ), where the 10% D.A. strain and  $R_u = 1$  criteria have occurred at the same time at the last (37th) cycle. For the specimens in which shear strain criterion was reached first, the

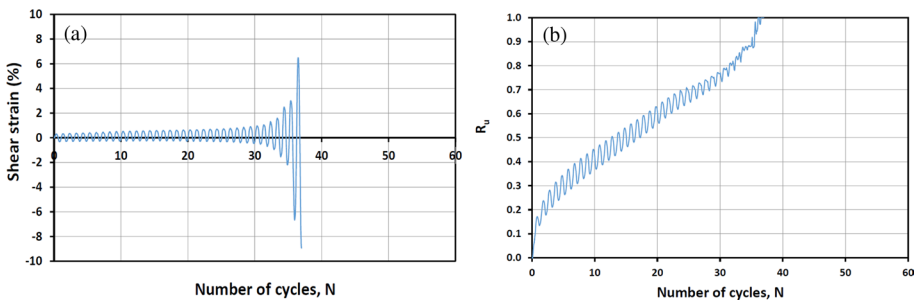


**Fig. 3** An example output for one of the tested silty sand specimens (Silica Sand with 5% YET silt tested at  $CSR = 0.1$ ,  $\sigma'_{vc} = 100$  kPa,  $D_r = 41.9\%$ ) **a** shear strain vs. the number of cycles (N), **b**  $R_u$  vs. N

average  $R_u$  value is calculated to be 0.93 for both Silica Sand-YET silt and Sile Sand 20/30-SI silt mixtures.

Some typical patterns of liquefaction can also be observed in Fig. 3. For instance, shear strains started to accumulate very slowly at initial stages of cyclic loading in Fig. 3a, then the rate of accumulation suddenly increased notably after about 32nd cycle, which corresponds to  $R_u > 0.8$  in Fig. 3b.

## 4 Results and discussion

### 4.1 Number of cycles to liquefaction and relative density relationship

Many of the previous literature considered one or two relative density values representing loose or medium dense states and conducted their cyclic triaxial or simple shear tests on specimens at those target relative density values to investigate the influence of various factors (e.g. FC, gradation, shape effects, stress history etc.). In this study however, tests were conducted over a relatively wide range of  $D_r$  values as much as the studied soils and employed specimen preparation technique permitted. It should also be reminded that no specific  $D_r$  values were targeted during the specimen preparation process in this study. Instead, specimens were deposited at “arbitrary”  $D_r$  values over a wide relative density range, which enabled authors to observe the relative density dependent trends (e.g. Figs. 4 and 5) discussed in the following sections of the

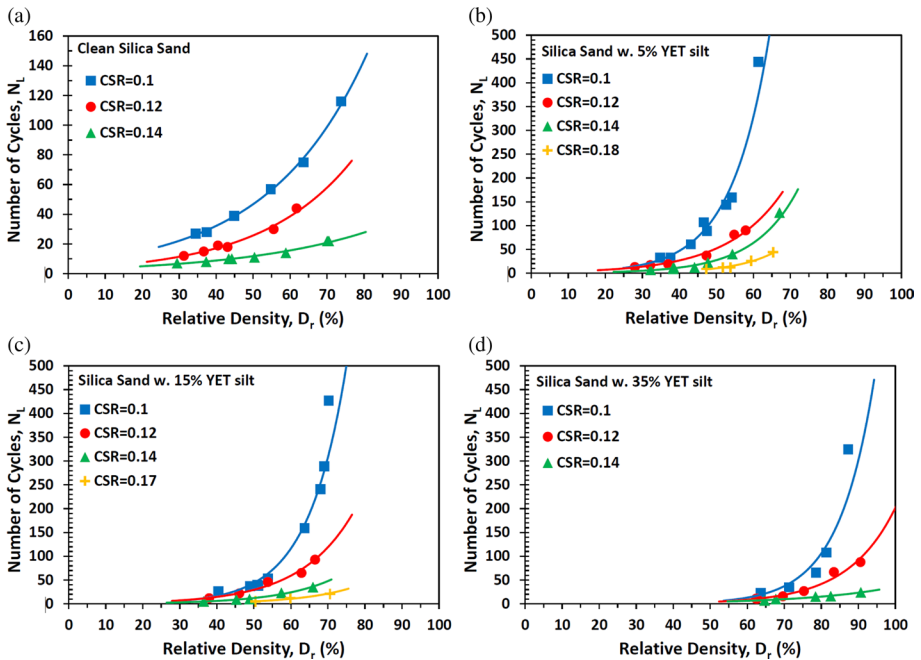


**Fig. 4** Change of the number of cycles to liquefaction ( $N_L$ ) with relative density ( $D_r$ ) at various CSR values for **a** a clean Silica sand, **b** Silica sand w. 5% YET silt, **c** Silica sand w. 15% YET silt, **d** Silica sand w. 35% YET silt



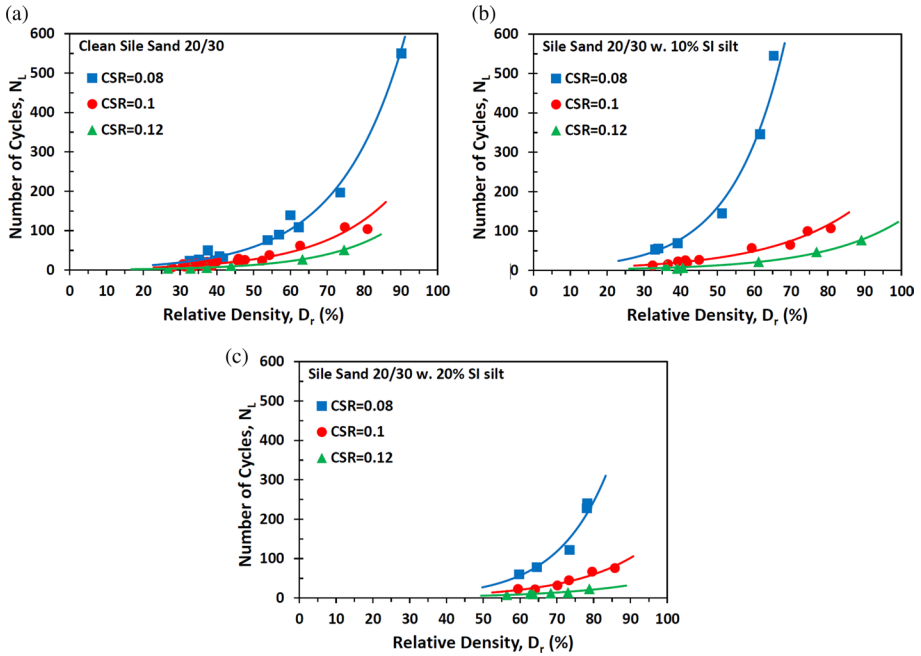


**Fig. 5** Change of the number of cycles to liquefaction ( $N_L$ ) with relative density ( $D_r$ ) at various CSR values for **a** clean Silty sand 20/30, **b** Silty sand w. 10% SI silt, **c** Silty sand w. 20% SI silt

paper. As explained in detail by Monkul et al. (2018), the achieved  $D_r$  of specimens prepared by automatic dry funnel deposition technique is a function of several factors including geometry and dimensions of the funnel, funnel raising speed, number of funnel extensions, type and grain size distribution of tested soils. Furthermore, Monkul and Yamamuro (2010) explained that densification of silty sand specimens during preparation either by tapping, vibrating or tamping to achieve a target  $D_r$  value could cause selective elimination of the “metastable” grain contacts between the sand and silt grains (i.e. weak grain contacts that can be easily destroyed by small additional forces). Hence, another reason for depositing and testing the specimens not at predetermined  $D_r$  values is because the densification process of silty sand specimens to target specific relative density values may cause disproportionate changes in their undrained response (Monkul and Yamamuro 2010).

The relationship between the number of cycles to liquefaction ( $N_L$ ) and relative density ( $D_r$ ) is plotted at various CSR values for clean Silica Sand in Fig. 4a, Silica Sand with 5% YET silt in Fig. 4b, Silica Sand with 15% YET silt in Fig. 4c, and Silica Sand with 35% YET silt in Fig. 4d. Note that the values in all of the figures correspond to  $D_r$  after consolidation. As expected, at a given CSR value the number of cycles to liquefaction increases with increasing relative density for all the soils, however the rate of increase in  $N_L$  decreases with increasing CSR value in Fig. 4. Same trends can also be observed for clean Silty Sand 20/30 in Fig. 5a, Silty Sand 20/30 with 10% SI silt in Fig. 5b, and Silty Sand 20/30 with 20% SI silt in Fig. 5c. Based on the data in Figs. 4 and 5, the relationship between  $N_L$  and  $D_r$  can be represented with an exponential function as shown in Eq. 1, which is also shown by the trend curves in the relevant figures.

$$N_L = c_1 \cdot \exp^{[c_2 \cdot Dr(\%)]} \quad (\text{at a given CSR}) \quad (1)$$

where  $c_1$  and  $c_2$  are the coefficients, which can be influenced by many factors including but not limited to the value of CSR, gradation, FC etc. and “exp” is the Euler’s number.

### 4.2 Cyclic stress ratio and number of cycles to liquefaction relationship

The change of number of cycles to liquefaction ( $N_L$ ) with CSR is plotted for the selected  $D_r$  values (based on Fig. 4) in a semi-log scale in Fig. 6 for clean Silica sand and its mixtures with YET silt at three fines contents (i.e. FC = 5%, 15% and 35%). Similarly, Fig. 7 shows the variation of  $N_L$  with CSR for clean Sile Sand 20/30 and its mixtures with SI silt (i.e. FC = 10%, 20%).

As an expected general trend,  $N_L$  increases with decreasing CSR for all soils. More specifically, Figs. 6a to 7c clearly show that at a given relative density, the relationship between  $N_L$  and CSR can be expressed by the power relationship shown in Eq. 2 for different clean and silty sand types, which is also shown by the trend lines in Figs. 6 and 7.

$$CSR = a \cdot N_L^{-b} \quad (\text{at a given } D_r) \quad (2)$$

where  $a$  and  $b$  are soil specific coefficients, which can be influenced by many factors including but not limited to the value of  $D_r$ , gradation, shape effects, mineralogy, FC etc. Note that Eq. 2 is not a new relationship and has been proposed in several other liquefaction studies as well (Idriss and Boulanger 2008; Moug et al. 2019). The coefficient of determination ( $R^2$ ) values for each curve in Figs. 6 and 7 representing Eq. 2 also indicate that the mentioned relationship is reasonably well established. It is also interesting to note that the basic form of Eq. 2 seems to work not only at a given  $D_r$  but also at a given void ratio ( $e_c$ ) as well according to some other experimental studies in literature(Wei and

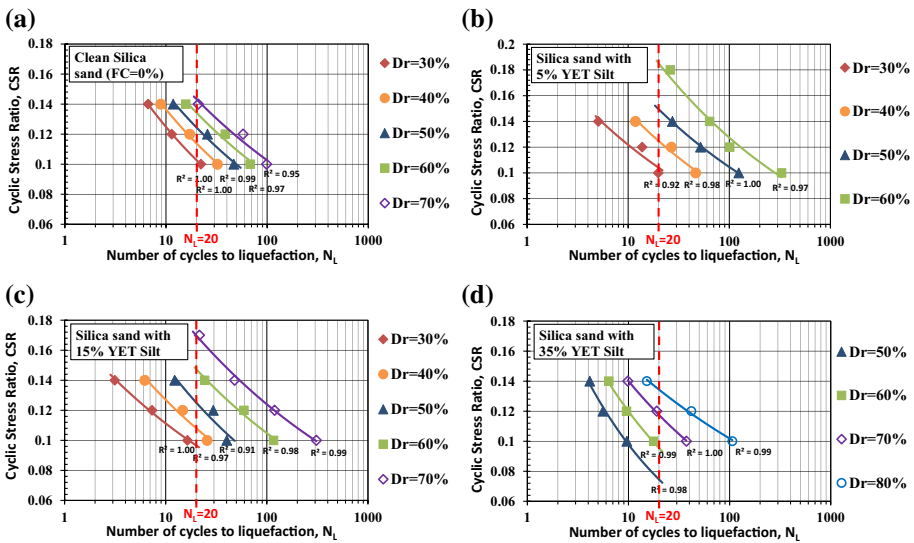
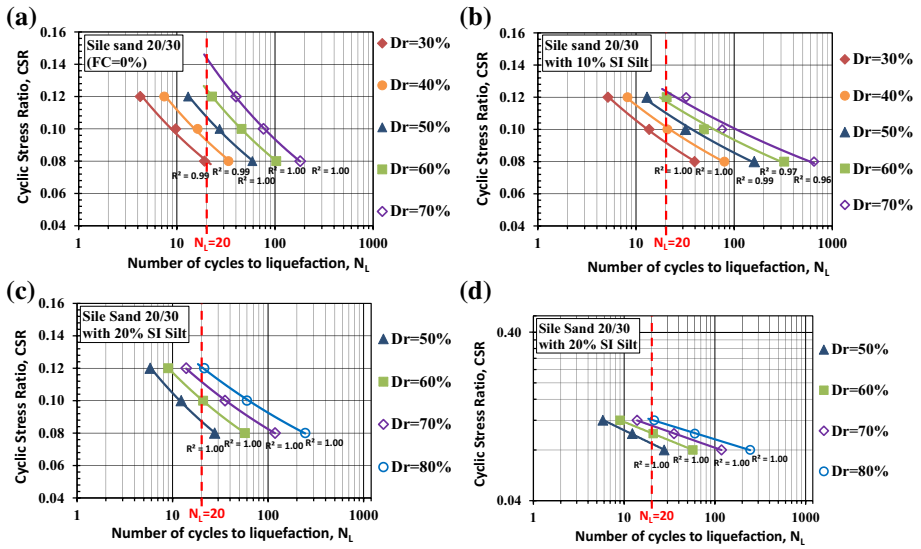


Fig. 6 Change of number of cycles to liquefaction ( $N_L$ ) with CSR at different  $D_r$  values for a clean Silica sand, b Silica sand w. 5% YET silt, c Silica sand w. 15% YET silt, d Silica sand w. 35% YET silt



**Fig. 7** Change of number of cycles to liquefaction ( $N_L$ ) with CSR at different  $D_r$  values for **a** clean Sile sand 20/30, **b** Sile sand w. 10% SI silt, **c** Sile sand w. 20% SI silt, **d** Sile sand w. 20% SI silt plotted on log–log scale

Yang 2019; Porcino et al. 2021). Moreover, Green and Terri (2005) discussed that there is an analogy between the CSR- $N_L$  relationship and the Palmgren–Miner damage hypothesis regarding metal fatigue during cyclic loading.

The concept of equivalent number of cycles ( $N_{eq}$ ) is commonly used to link the duration of the earthquake loading at the site (which is irregular in time) with the cyclic element tests performed in the laboratory (which typically involves uniform cyclic loading in time) (Seed et al. 1975). The value of  $N_{eq}$  is known to be related with the moment magnitude ( $M_w$ ) of earthquakes (Seed et al. 1975; Youd et al. 2001; Idriss and Boulanger 2008), although additional factors including depth in the soil profile and site to source distance can also be involved (Liu et al. 2001; Green and Terri 2005; Lasley et al. 2017). Therefore, the magnitude scaling factor (MSF), which is commonly used in the simplified liquefaction assessment methods, can be represented in the basic form of Eq. 3 given below (Boulanger and Idriss 2007; Idriss and Boulanger 2008; Ulmer et al. 2022), where  $N_{eq-Mw=7.5}$  correspond to the number of uniform stress cycles for  $M_w=7.5$  earthquake.

$$MSF = \frac{CSR}{CSR_{M_w=7.5}} = \left( \frac{N_{eq}}{N_{eq-M_w=7.5}} \right)^{-b} \tag{3}$$

Equation 3 indicates that magnitude scaling factor is indeed a function of the parameter  $b$  in Eq. 2. The  $b$  values of the tested soils in this study are determined from the trend curves plotted in Figs. 6 and 7 based on Eq. 2. It is worth to mention that the parameter  $b$  in Eqs. 2 and 3 corresponds to the slope of the CSR- $N_L$  line if Figs. 6 and 7 have been plotted on a log–log scale. According to some analyses in literature; CSR- $N_L$  relationship may become non-linear especially at low number of cycles (i.e.  $N_L < 10$ ) for the sands at dense to very dense states (i.e.  $D_r \geq 75\%$ ) even on log–log scale (Ulmer et al. 2022). However, for all the specimens plotted in Figs. 6 and 7, the CSR- $N_L$  relationship

becomes entirely linear on log–log scale for the studied range, indicating a constant  $b$  parameter for a given  $D_r$ . As an example, Fig. 7d shows the same data with Fig. 7c if plotted on a log–log scale, clearly illustrating the linear relationship (constant  $b$  value) between CSR and  $N_L$  for the soils and testing conditions in this study. The reason why authors preferred plotting Figs. 6 and 7 on a semi-log scale is simply because the corresponding trend curves have more space in-between (i.e. aesthetic reasons).

The change of parameter  $b$  with relative density of the tested specimens is shown in Fig. 8a and b for Silica sand—YET silt mixtures and Sile Sand 20/30—SI silt mixtures respectively. Different trends were observed in Fig. 8a; for clean Silica Sand,  $b$  values slightly decrease with increasing  $D_r$ , whereas the value of  $b$  seems to be insensitive to  $D_r$  for sand with 5% silt. No clear trend was observed for sand with 15% silt, while  $b$ – $D_r$  relationship was most sensitive to  $D_r$  value for the sand with 35% silt (i.e. the  $b$  value drops from 0.39 at  $D_r=50\%$  to 0.17 at  $D_r=80\%$ ). It was also observed that with few exceptions, most  $b$  values for the Silica sand—YET silt mixtures are located between  $b=0.2$  and  $0.3$  boundaries shown by dashed lines in Fig. 8a.

Different trends were also observed in Fig. 8b regarding the Sile sand 20/30—SI silt mixtures. It is clear that parameter  $b$  for clean Sile Sand is equal to 0.27 regardless of its relative density (i.e.  $b$  is insensitive to  $D_r$  for clean Sile sand). Whereas for silty sands (FC = 10% and 20%) in Fig. 8b, the value of  $b$  decreases gradually with increasing  $D_r$ . Similar to Fig. 8a  $b$ – $D_r$  relationship was most sensitive to  $D_r$  value at relatively high FC values (i.e. at FC = 20% in Fig. 8b).  $b=0.15$  and  $0.3$  boundaries were also shown by dashed lines in Fig. 8b, where most  $b$  values for the Sile sand 20/30—SI silt mixtures are located in between.

Observations on Fig. 8 are also important because the  $b$  values reported in the literature were typically calculated based on the experimental response of clean sands, while much less data were available on the  $b$  values for silty sands. For instance, Idriss and Boulanger (2008) have considered  $b=0.34$  as a representative value based on the cyclic

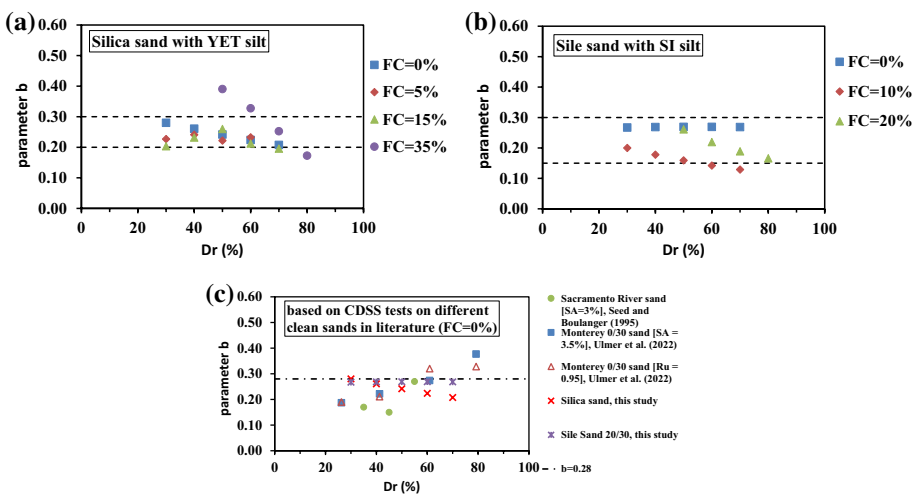


**Fig. 8** Variation of parameter  $b$  in Eqs. 2 and 3 with relative density for the tested soils: **a** Silica sand-Yet silt mixtures, **b** Sile sand 20/30-SI silt mixtures, **c**  $b$ – $D_r$  relationship for different clean sands in literature

triaxial tests on clean Niigata Sand (i.e. FC=0%) performed by Yoshimi et al. (1984) and consequently proposed Eq. 4 to calculate MSF for engineering practice.

$$MSF = 6.9 \exp\left(-\frac{M_w}{4}\right) - 0.058 \leq 1.8 \quad (4)$$

In a later study, Boulanger and Idriss (2014) made detailed analyses regarding parameter  $b$  based on the experimental data in literature. Accordingly, the  $b$  values for clean sands are quite variable depending on the magnitude of  $D_r$  and conditions at the site. For instance, based on the data of Okamura et al. (2003) by cyclic triaxial tests on frozen undisturbed samples,  $b$  value could range from 0.13 to 0.54. The relationship between parameter  $b$  and  $D_r$  is rather complicated as already discussed for the tested soils in Fig. 8a and b. Four different clean sand data are compiled from the literature in Fig. 8c, all originally performed by CDSS tests. All the specimens in Fig. 8c were consolidated to 100 kPa vertical effective stress ( $\sigma'_{vc} = 100$  kPa) except the Sacramento River Sand (Boulanger and Seed 1995), for which  $\sigma'_{vc}$  was 207 kPa. Different trends could be observed in Fig. 8c, such as parameter  $b$  increases with increasing  $D_r$  (e.g. Monterey 0/30 Sand); parameter  $b$  decreases slightly with increasing  $D_r$  (e.g. Silica Sand); no clear trend between  $b$  and  $D_r$  (e.g. Sacramento River Sand), and parameter  $b$  remains constant with increasing  $D_r$  (e.g. Sile Sand 20/30). Figure 8c further reveals that parameter  $b$  is also dependent on sand type (i.e. different clean sands may have different  $b$  values at a given  $D_r$ ).

Moreover, some researchers proposed alternative approaches to determine parameter  $b$ . For instance, Ulmer et al. (2022) proposed that CSR- $N_L$  curves can be obtained by using dissipated energy approach and recommended a representative value of  $b=0.28$  by using modulus reduction and damping curves. The parameter  $b$  recommended by Ulmer et al. (2022) which is independent of  $D_r$  is also shown in Fig. 8c by the dashed lines (i.e.  $b=0.28$ ). Accordingly, the representative value of  $b=0.28$  is quite close to the  $b$  values calculated for the Sile Sand 20/30 (Fig. 8c), however for other clean sands,  $D_r$  dependent  $b$  parameter concept may result in notably different  $b$  values.

Figure 8 further reveals that the parametric values of  $b$  parameter for silty sands at different fines contents (Fig. 8a, b) are comparable with that of the clean sands (Fig. 8c). More specifically, the range of  $b$  values for the Silica sand – YET silt mixtures in Fig. 8a and Sile sand 20/30 – SI silt mixtures in Fig. 8b are quite similar to the parameter  $b$  range observed in Fig. 8c for different clean sands tested in literature.

### 4.3 Cyclic resistance ratio and relative density relationship

Cyclic resistance ratio (CRR) is a commonly used parameter to quantify the liquefaction resistance of soils. In this study, CSR value causing the liquefaction of specimens in 20 uniform cycles is considered as the CRR. Corresponding  $N_L=20$  references are shown by red dashed lines in Figs. 6 and 7.  $N_{cq}=20$  would approximately correspond to a  $M_w=7.8$  earthquake similar to the Kahramanmaraş–Pazarcık earthquake sequence in Turkey, occurred on February 6th, 2023 and devastated the region (Ozener et al. 2024).

For the two clean sands tested in this study (Silica and Sile sands), the change of CRR with relative density is shown in Fig. 9a. Accordingly, there is a linear relationship between the CRR and  $D_r$  as shown in Eq. 5 below, where  $c_3$  and  $c_4$  are soil specific coefficients. Equation 5 indicates that CRR increases linearly with increasing  $D_r$  for the studied range.

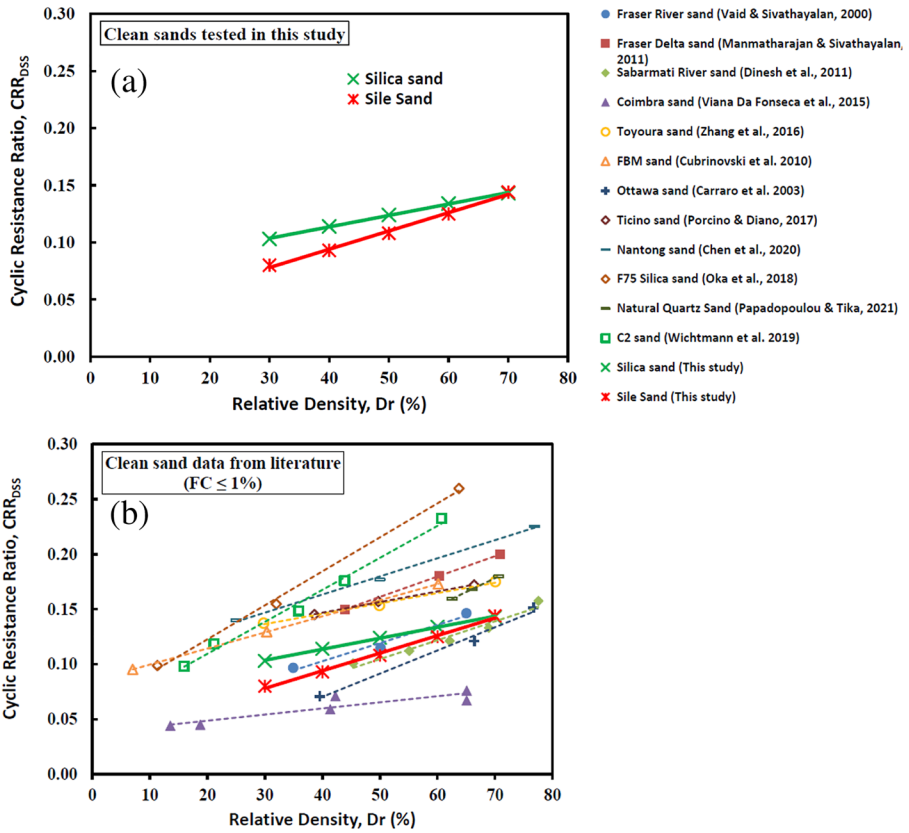


Fig. 9 Cyclic Resistance Ratio (CRR)– $D_r$  relationship for clean sands. **a** Clean sands tested in this study, **b** various clean sands from literature ( $FC \leq 1\%$ )

$$CRR = c_3 \cdot D_r(\%) + c_4 \tag{5}$$

The trend line for Silica sand is located above the line for Sile sand 20/30 in Fig. 9a, indicating a greater liquefaction resistance when two sands are compared at the same  $D_r$ , especially for loose to medium dense states. However, the two lines tend to merge eventually towards the dense state and the two clean sands have the same liquefaction resistance at  $D_r=70\%$  (Fig. 9a).

In order to verify the linear relationship in Eq. 5 for different soils, relevant data for other clean sands in literature are plotted in Fig. 9b with the dashed lines representing Eq. 5 for the individual soils. Note that the liquefaction resistance obtained by cyclic triaxial tests ( $CRR_{CTX}$ ) in literature were converted to their cyclic simple shear equivalent values ( $CRR_{CDSS}$ ) by using Eq. 6, where  $C_r$  is the correction coefficient. Previous studies reported that the value of  $C_r$  is indeed influenced by several factors including  $D_r$ , confining stress and initial static shear stress ratio (Vaid and Sivathayalan 1996; Nong et al. 2021). The correction coefficient ( $C_r$ ) is chosen as 0.7 for the data in Fig. 9b based on practical recommendation by Kramer (1996). This is because the original triaxial data (CRR

$C_{TX}$ ) also confirm the linear relationship given in Eq. 5, and CRR values in Fig. 9b are not intended for direct numerical comparison as differences in various factors including effective consolidation stress, specimen preparation methods etc. would also affect the absolute CRR values. Moreover, any possible change in  $C_r$  with the mentioned factors (including  $D_r$ , confining stress etc.) requires an elaborate calibration process involving CTX and CDSS tests conducted on each sand type, which is not available in literature.

$$CRR_{CDSS} = C_r \cdot CRR_{CTX} \quad (6)$$

Nevertheless, Fig. 9b reveals that Eq. 5 works very well for various clean sands compiled from literature, including Fraser river sand (Vaid and Sivathayalan 2000), Fraser Delta sand (Manmatharajan and Sivathayalan 2011), Sabarmati River sand (Dinesh et al. 2011), Coimbra sand (Viana Da Fonseca et al. 2015), Toyoura sand (Zhang et al. 2016), FBM sand (Cubrinovski et al. 2010), Ottawa sand (Carraro et al. 2003), Ticino sand (Porcino and Diano 2017), Nantong sand (Chen et al. 2020), F75 Silica sand (Oka et al. 2018), Natural Quartz sand (Papadopoulou and Tika 2021), C2 sand (Wichtmann et al. 2019). Note that the good performance of Eq. 5 shown in Fig. 9 is discussed only for the studied  $D_r$  range (i.e.  $D_r < 80\%$ ), and it is possible that the relationship between CRR and  $D_r$  may become nonlinear (i.e. curved up) at greater  $D_r$  values.

It is also important to verify applicability of Eq. 5 for silty sands. CRR- $D_r$  relationship for silty sands has been shown in Fig. 10a and b for silty sands with  $FC \leq 15\%$  and  $15\% < FC \leq 35\%$ , respectively. As seen in Fig. 10, Eq. 5 works not only for the silty sands tested in this study, but also works for various other silty sands tested in literature.

#### 4.4 Liquefaction resistance–fines content–relative density relationship

As already mentioned in the introduction section, several different trends are observed in literature regarding the influence of fines content on liquefaction resistance of sands. Moreover, some of those trends were conflicting with each other, such as liquefaction resistance of a sand increases with FC or vice versa, even though relative density was the comparison parameter (i.e. liquefaction resistances were compared at the same  $D_r$  value).

The variation of CRR with relative density is shown in Fig. 11a for Silica sand with different amount of YET silt. This figure reveals some very important observations regarding the fines content effect on liquefaction resistance. The most important one is that the effect of FC on liquefaction resistance is not unique but rather depends on the value of relative density. For instance, clean sand and the silty sand with 5% FC has the same liquefaction resistance at  $D_r = 30\%$ . However, as the  $D_r$  increases, sand with 5% FC has greater liquefaction resistance compared to the clean sand. Moreover, the difference between the liquefaction resistance of two soils (i.e. clean sand and sand with 5% FC) becomes systematically greater as the  $D_r$  increases because of the diverging trend of corresponding lines with  $D_r$  (Fig. 11a). Hence, at  $D_r = 60\%$  the  $CRR_{FC=5\%}$  is significantly greater than  $CRR_{FC=0\%}$ . As the fines content increases from 5 to 15%, and from 15 to 35% the CRR lines shift down, indicating a decreasing liquefaction resistance as the FC increases from 5 to 35%. Note that the silty sand with  $FC = 35\%$  is weakest soil in Fig. 11a in terms of liquefaction resistance at a given  $D_r$ .

Change of CRR with  $D_r$  for Sile sand 20/30 with SI silt is shown in Fig. 11b. This figure also shows that effect of FC on liquefaction resistance depends on  $D_r$ . Another important finding observed in Fig. 11 is that the clean sand CRR- $D_r$  line may be crossed by a silty sand CRR- $D_r$  line. For instance, in Fig. 11a 15% silty sand line crossed the clean

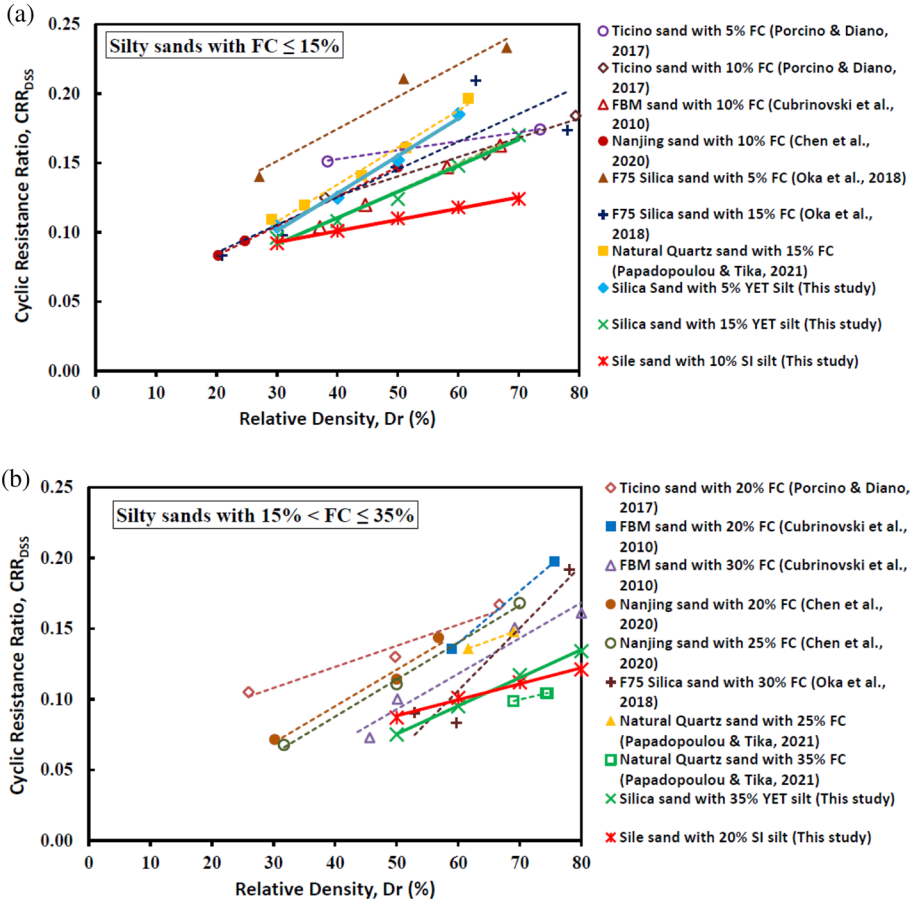


**Fig. 10** Cyclic Resistance Ratio (CRR)– $D_r$  relationship for different silty sands **a** silty sands with  $FC \leq 15\%$ , **b** silty sands with  $15\% < FC \leq 35\%$

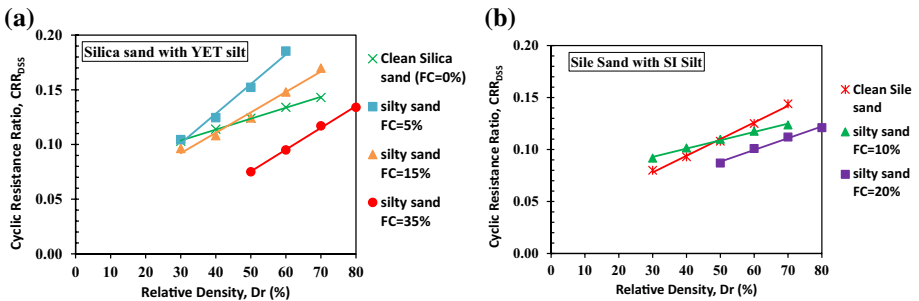


**Fig. 11** Cyclic Resistance Ratio (CRR)– $D_r$ –Fines Content (FC) relationship for **a** Silica sand-YET silt mixtures, **b** Sile sand 20/30- SI silt mixtures



sand line at an approximate relative density value of 42%, while 10% silty sand line in Fig. 11b crossed the clean sand line at an approximate relative density value of 50%. The mentioned “crossing effect” is a very important finding, indicating that different FC-liquefaction resistance trends may all be valid even for the same soil pair (i.e. the same clean and silty sand) depending on the value of  $D_r$ . For example, for the silty sand with 15% FC in Fig. 11a; even though compared at the same relative density value,  $CRR_{\text{silty sand}} > CRR_{\text{clean sand}}$  if relative density is greater than 42%, however  $CRR_{\text{clean sand}} > CRR_{\text{silty sand}}$  if relative density is smaller than 42%. Similarly, for silty sand with 10% FC in Fig. 11b;  $CRR_{\text{clean sand}} > CRR_{\text{silty sand}}$  if relative density is greater than 50%, however  $CRR_{\text{silty sand}} > CRR_{\text{clean sand}}$  if relative density is smaller than 50%.

The conflicting influence of  $D_r$  on the FC-liquefaction resistance comparisons between clean and silty sands or the “crossing effect” mentioned above can be better visualized in Fig. 12a and b for Silica and Sile sands respectively. If three different  $D_r$  slices are taken from Fig. 11a and plotted in Fig. 12a, one can see three different comparison trends for the clean sand and silty sand with 15% FC:  $CRR_{\text{clean sand}} > CRR_{\text{silty sand}}$  at  $D_r=30\%$ ,  $CRR_{\text{clean sand}} = CRR_{\text{silty sand}}$  at  $D_r=42\%$ ,  $CRR_{\text{clean sand}} < CRR_{\text{silty sand}}$  at  $D_r=60\%$ . Similarly, if three  $D_r$  slices are taken from Fig. 11b and plotted in Fig. 12b, one can see three different comparison trends for the clean sand and silty sand with 10% FC:  $CRR_{\text{clean sand}} < CRR_{\text{silty sand}}$  at  $D_r=30\%$ ,  $CRR_{\text{clean sand}} = CRR_{\text{silty sand}}$  at  $D_r=50\%$ ,  $CRR_{\text{clean sand}} > CRR_{\text{silty sand}}$  at  $D_r=70\%$ .

Figure 12 reveals that the different (and conflicting) influence of FC on liquefaction resistance is indeed influenced by the value of relative density. More explicitly, for some soils  $D_r$ -CRR lines may cross each other as seen in Fig. 11, which could potentially change the FC-liquefaction resistance comparison of the clean versus silty sands. To authors’ knowledge, the mentioned “crossing effect” were neither explicitly reported nor discussed previously in literature, even though there had been several valuable studies on the subject over the years. Hence it is important to examine whether similar crossings of  $D_r$ -CRR lines could also be observed for different soils tested by other researchers. Figure 13a shows the  $D_r$ -CRR relationship for the FBM sand tested by Cubrinovski et al. (2010), where a clear crossing could be observed this time for the two silty sands (FC = 10% and FC = 20%) at around  $D_r \approx 67\%$ .  $D_r$ -CRR relationship for the F75 Silica sand tested by Oka et al. (2018)

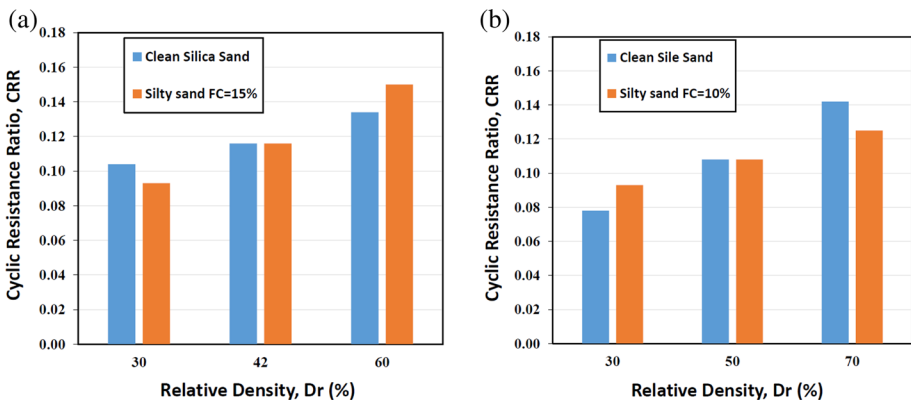


**Fig. 12** Comparison of the liquefaction resistance of clean and silty sands at different relative densities: **a** clean Silica sand versus silty sand with 15% YET silt, **b** clean Sile sand 20/30 versus silty sand with 10% SI silt

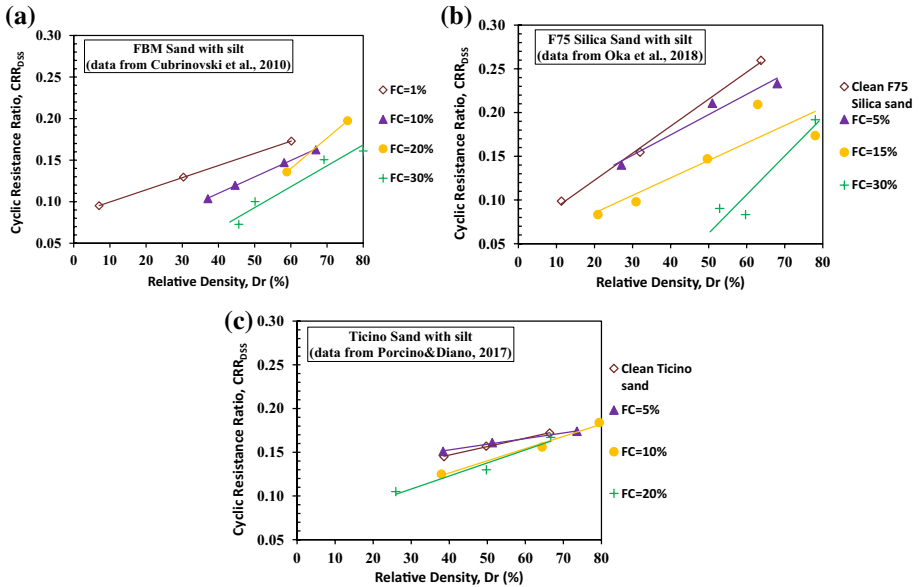


**Fig. 13** Cyclic Resistance Ratio (CRR)– $D_r$ –Fines Content (FC) relationship for different soils in literature. **a** FBM sand-silt mixtures, **b** F75- silt mixtures, **c** Ticino sand-silt mixtures

is plotted in Fig. 13b, where a crossing between clean and silty sand with 5% FC could be observed at around  $D_r \approx 27\%$ . Figure 13c shows the response of Ticino sand with different amounts of silt tested by Porcino and Diano (2017). Several different crossings could also be observed in Fig. 13c, however because the trend lines are relatively close to each other, it is difficult to comment on the intersection values.

Consequently, the “crossing effect” can also be observed for different sands and silty sands tested in literature. Moreover, the data from literature confirm that the effect of FC on liquefaction resistance of sands is not uniform but depends on the value of relative density. Explaining the underlying reasons behind the complex effect of  $D_r$  on liquefaction resistance and the “crossing effect” is not easy and requires further and extensive research tasks, which are beyond the limits of this study. These include but not limited to assessing the micro-fabric of clean and silty sands with varying FC achieved before cyclic loading at different relative density values. For instance, Yamamuro et al. (2008) preserved the microstructure of Nevada sand specimens having different FC with epoxy impregnation and quantified the stable and unstable grain contacts via multiple SEM micrographs to discuss the monotonic undrained behavior of Nevada sand. In the same study contact stability ratio ( $S$ ) was proposed based on the grain contact structure of silty sands, which is shown to be influential on the undrained monotonic response.

Theoretical explanations may also be linked to the critical state soil mechanics framework. It is known that the position of the initial state of sands in the void ratio-mean effective stress space and its distance from the critical state line (CSL) (i.e. state parameter,  $\psi$ ) have been previously shown to strongly influence the cyclic resistance of sands both by experimental (Stamatopoulos 2010; Porcino et al. 2021) and numerical studies (Kolapalli et al. 2023). Considering that the location and slope of the CSL are affected by the fines content (Been and Jefferies 1985; Papadopoulou and Tika 2008; Dash et al. 2010;

Stamatopoulos 2010; Kwa and Airey 2017; Wei and Yang 2019), it is possible that the “crossing effect” demonstrated in this study may be linked with the evolution of CSL for clean and silty sands (i.e. the change of its location and/or slope due to FC) together with the amount of change in initial state parameter values for different relative densities. Note that at a given relative density value, the initial state of a clean and silty sand in the void ratio-mean effective stress space is also influenced by the  $e_{\max}$  and  $e_{\min}$  of the clean and silty sands being considered. Nevertheless, these extensive research tasks involving the micro-structure grain contact quantification and critical state soil mechanics could be a matter of future research.

#### 4.5 Importance of the “crossing effect” and its implications for engineering practice

Adopting the concept of crossing effect to geotechnical engineering practice is also an important aspect. Indeed, this is a very complicated task, because the dynamics of the crossing effect is soil specific and requires an elaborate laboratory investigation to determine. This could be better seen in Table 2, where the crossing effect patterns for different soils are summarized. Several important observations could be drawn from Table 2; the first one is that the “crossing effect” may occur between clean and silty sand pairs (e.g. clean and silty Sile, Silica, F75 sands) as well as between two silty sand pairs involving the same base sand but having different FC (e.g. silty FBM sands, and silty Ticino sands). Hence the FC values for which the crossing may occur depends on the soils considered. The second one is that the “crossing effect” may occur over a wide relative density range, which is between 27 and 73% for the soils analyzed in Table 2, implying that loose, medium dense and dense soils may all be subjected to the crossing effect depending on the conditions. Crossing  $D_r$  value is expected to be influenced by many factors including but not limited to the gradation properties, type and mineralogy of the soils, FC, shape effects etc. Another interesting observation from Table 2 is the possibility of opposite trends after crossing. More specifically, cyclic resistance of silty sand become greater than that of the clean sand after the crossing for Silica sand, while cyclic resistance of silty sand become smaller than that of the clean sand after the crossing for Sile and F75 sands. Whereas, for crossings between two silty sands having different FC, the one with greater FC seems to have greater cyclic resistance than the other one after the crossing occurs (e.g. silty FBM and silty Ticino sands). However, more research and data on other silty sands are needed to investigate whether this is the only trend possible for the silty sand pairs.

The “crossing effect” is also quite important for geotechnical engineering practice, because it implies that during an earthquake, even reverse trends are possible between the very same clean and silty sand pair having the same  $D_r$  at a site depending on the value of  $D_r$  (i.e. the very same silty sand could have greater liquefaction resistance than the clean sand or vice versa depending on  $D_r$ ). However, due to its complex nature (which is discussed based on the information in Table 2), it is not an easy task to immediately develop a way to implement its usage in geotechnical engineering practice. However, future research involving both laboratory and in-situ testing on different soils could make this possible. In fact, a very recent study of the first author, involving Seismic Cone Penetration Tests (SCPT) on Silica sand-silt mixtures deposited in a rigid aluminum box, also revealed that Cyclic Resistance Ratio ( $CRR_{7.5}$ ) vs. normalized shear wave velocity ( $V_{s1}$ ) curves could also show a trend similar to the “crossing effect” introduced in this paper. In that study,  $CRR_{7.5} - V_{s1}$  curves for the sand-silt mixtures having different soil type indices ( $I_c$ ) were shown to cross each other at around  $V_{s1} = 170$  m/s (Ecemis et al. 2024).

**Table 2** Summary of the crossing effect observed for different soils

Fig. No	Crossing soil 1	Crossing soil 2	Approximate $D_r$ at crossing (%)	Trend after crossing
Fig. 11a	Clean Silica sand	Silty Silica sand (15% FC)	42	Liquefaction resistance of silty sand becomes greater than that of the clean sand
Fig. 11a	Clean Silica sand 20/30	Silty Silica sand (5% FC)	30	Liquefaction resistance of silty sand becomes greater than that of the clean sand
Fig. 11b	Clean Silt sand	Silty Silt sand (10% FC)	50	Liquefaction resistance of silty sand becomes smaller than that of the clean sand
Fig. 13a	Silty FBM sand (FC = 10%)	Silty FBM sand (20% FC)	67	Liquefaction resistance of silty sand with 20% FC becomes greater than that of the silty sand with 10% FC
Fig. 13b	Clean F75 sand	Silty F75 sand (5% FC)	27	Liquefaction resistance of silty sand becomes smaller than that of the clean sand
Fig. 13c	Silty Ticino sand (FC = 5%)	Silty Ticino sand (10% FC)	73	Liquefaction resistance of silty sand with 10% FC becomes greater than that of the silty sand with 5% FC

More specifically, for  $V_{s1} > 170$  m/s, liquefaction resistance of the tested sand-silt mixtures was shown to increase with increasing  $I_c$  (i.e. silty sand has greater liquefaction resistance than the clean sand at a given  $V_{s1} > 170$  m/s), whereas the opposite trend was observed for  $V_{s1} < 170$  m/s (i.e. silty sand has smaller liquefaction resistance than the clean sand at a given  $V_{s1} < 170$  m/s) (Ecemis et al. 2024).

## 5 Summary and conclusions

In this study the influence of relative density on the liquefaction resistance of clean and silty sands is studied via CDSS tests. Even though  $D_r$  is a very traditional density index parameter commonly used in geotechnical earthquake engineering research and practice, the findings of this experimental study reveal that its effect on liquefaction mechanism of sands is rather complex.

In the initial part of the study, the relationship between relative density and number of cycles to liquefaction was investigated. It was observed that there is an exponential relationship between the two parameters as shown in Eq. 1. In the second part of the study a relatively well-known relationship between  $N_L$  and CSR (Eq. 2) was revisited and confirmed by the experimental results in this study. It was observed that the value of parameter  $b$  in Eq. 2, which can also be used to calculate MSF, is also influenced by the relative density. However, different trends are possible regarding the  $b$ - $D_r$  relationship. More specifically, parameter  $b$  may increase, decrease or remain constant with an increase in  $D_r$  depending on the soil type (see Fig. 8). With few exceptions, most  $b$  values for the Silica sand-YET silt mixtures tested in this study remain between 0.2 and 0.3, while the ones for the Sile sand 20/30-SI silt mixtures remain between 0.15 and 0.3. It was found that  $b$ - $D_r$  relationship was most sensitive to  $D_r$  value at relatively high fines content (i.e. FC=35% for YET silt mixtures, FC=20% for SI silt mixtures).

In the third part of the study, the relationship between cyclic resistance ratio and relative density was investigated. It was shown that there is a linear relationship between CRR and  $D_r$  for both clean (Fig. 9) and silty sands (FC ≤ 35%) (Fig. 10) as shown in Eq. 5 within the studied relative density range.

In the last part of the study, liquefaction resistance-fines content and relative density relationship was investigated. It was found that the effect of FC on liquefaction resistance may not be unique but rather depends on the value of  $D_r$ . This is because  $D_r$ -CRR line of a clean sand may be crossed by the  $D_r$ -CRR line of a silty sand (Fig. 11). This important finding revealed first time in literature is named as the “crossing effect”. Accordingly, for the very same clean and silty sand pair having the same the same  $D_r$ , during an earthquake  $CRR_{\text{clean sand}}$  may be greater than  $CRR_{\text{silty sand}}$ ; or  $CRR_{\text{clean sand}}$  may be equal to  $CRR_{\text{silty sand}}$ ; or  $CRR_{\text{clean sand}}$  may be smaller than  $CRR_{\text{silty sand}}$  depending on the magnitude of relative density (Fig. 12). Moreover, even if a single trend exists between a clean and silty sand pair, the level of FC influence on liquefaction resistance could still be notably affected by the magnitude of  $D_r$ . As an example, the difference between the liquefaction resistances of clean and silty sand with 5% FC in Fig. 11a became systematically greater as the  $D_r$  increased.

Consequently, it was shown that not only the level of FC influence (i.e. magnitude of  $\Delta CRR$  due to fines content) but also the trend of FC influence (i.e. +  $\Delta CRR$ ,  $\Delta CRR = 0$ , or -  $\Delta CRR$  due to fines content) on cyclic liquefaction resistance of sands could be surprisingly affected by the value of  $D_r$ . The latter finding is quite important for engineering

practice because it implies that even reverse trends (positive or negative effect of silt content on CRR) could be observed between the very same clean and silty sand pair having the same  $D_r$  at a site depending on the magnitude of relative density. Geotechnical engineers should be cautious about the complex and potentially conflicting influence of relative density on liquefaction resistance of clean versus silty sands.

**Acknowledgements** Some CDSS tests were performed by the former graduate student Sena Begüm Kendir, which is greatly appreciated by the authors.

**Author contributions** All authors contributed to the study conception and design. Mehmet Murat Monkul: Supervision, Conceptualization, Methodology, Writing the original draft, Writing; Yunus Emre Tütüncü: Investigation, Validation, Methodology, Writing – review & editing. All authors read and approved the final manuscript.

**Funding** Open access funding provided by the Scientific and Technological Research Council of Türkiye (TÜBİTAK). The authors declare that no financial support was received during the preparation of this study.

## Declarations

**Conflict of interests** The authors have no relevant financial or non-financial interests to disclose.

**Data availability** The data of the experiments used in the figures and analysed during the current study are available from the corresponding author on reasonable request.

**Open Access** This article is licensed under a Creative Commons Attribution 4.0 International License, which permits use, sharing, adaptation, distribution and reproduction in any medium or format, as long as you give appropriate credit to the original author(s) and the source, provide a link to the Creative Commons licence, and indicate if changes were made. The images or other third party material in this article are included in the article's Creative Commons licence, unless indicated otherwise in a credit line to the material. If material is not included in the article's Creative Commons licence and your intended use is not permitted by statutory regulation or exceeds the permitted use, you will need to obtain permission directly from the copyright holder. To view a copy of this licence, visit <http://creativecommons.org/licenses/by/4.0/>.

## References

- Amini F, Qi GZ (2000) Liquefaction testing of stratified silty sands. *J Geotech Geoenviron Eng* 126:208–217
- Bahadori H, Ghalandarzadeh A, Towhata I (2008) Effect of non plastic silt on the anisotropic behavior of sand. *Soils Found* 48:531–545. <https://doi.org/10.3208/sandf.48.531>
- Been K, Jefferies MG (1985) A state parameter for sands. *Geotechnique* 35:99–112
- Bhattacharya S, Hyodo M, Goda K et al (2011) Liquefaction of soil in the Tokyo Bay area from the 2011 Tohoku (Japan) earthquake. *Soil Dyn Earthq Eng* 31:1618–1628. <https://doi.org/10.1016/j.soildyn.2011.06.006>
- Boominathan A, Rangaswamy K, Rajagopal, (2010) Effect of non-plastic fines on liquefaction resistance of Gujarat sand. *Int J Geotech Eng* 4:241–253. <https://doi.org/10.3328/IJGE.2010.04.02.241-253>
- Boulanger RW, Idriss IM (2007) Evaluation of cyclic softening in silts and clays. *J Geotech Geoenviron Eng* 133:641–652. [https://doi.org/10.1061/\(ASCE\)1090-0241\(2007\)133:6\(641\)](https://doi.org/10.1061/(ASCE)1090-0241(2007)133:6(641))
- Boulanger RW, Idriss IM (2014) CPT and SPT based liquefaction triggering procedures, Report No: UCD/CGM-14/01. University of California, Davis
- Boulanger RW, Seed RB (1995) Liquefaction of sand under bidirectional monotonic and cyclic loading. *J Geotech Eng* 121:870–878
- Bray JD, Sancio RB, Durgunoglu T et al (2004) Subsurface characterization at ground failure sites in Adapazari, Turkey. *J Geotech Geoenviron Eng* 130:673–685. [https://doi.org/10.1061/\(ASCE\)1090-0241\(2004\)130:7\(673\)](https://doi.org/10.1061/(ASCE)1090-0241(2004)130:7(673))
- Carraro JAH, Bandini P, Salgado R (2003) Liquefaction resistance of clean and nonplastic silty sands based on cone penetration resistance. *J Geotech Geoenviron Eng* 129:965–976. [https://doi.org/10.1061/\(ASCE\)1090-0241\(2003\)129:11\(965\)](https://doi.org/10.1061/(ASCE)1090-0241(2003)129:11(965))

- Chen G, Wu Q, Zhao K, et al (2020) A binary packing material-based procedure for evaluating soil liquefaction triggering during earthquakes. *J Geotech Geoenviron Eng* 146. [https://doi.org/10.1061/\(ASCE\)GT.1943-5606.0002263](https://doi.org/10.1061/(ASCE)GT.1943-5606.0002263)
- Choo H, Burns SE (2015) Shear wave velocity of granular mixtures of silica particles as a function of finer fraction, size ratios and void ratios. *Granul Matter* 17:567–578. <https://doi.org/10.1007/s10035-015-0580-2>
- Cubrinovski M, Ishihara K (1999) Empirical correlation between SPT-N value and relative density for sandy soils. *Soils Found* 39:61–71
- Cubrinovski M, Ishihara K (2002) Maximum and minimum void ratio characteristics of sands. *Soils Found* 42:65–78. [https://doi.org/10.3208/sandf.42.6\\_65](https://doi.org/10.3208/sandf.42.6_65)
- Cubrinovski M, Rees S, Bowman E (2010) Chapter 6: effects of non-plastic fines on liquefaction resistance of sandy soils. In: Garevski M, Ansal A (eds) *Earthquake engineering in Europe*. Springer, London, pp 125–144
- Dash HK, Sitharam TG, Baudet BA (2010) Influence of non-plastic fines on the response of a silty sand to cyclic loading. *Soils Found* 50:695–704. <https://doi.org/10.3208/sandf.50.695>
- Dinesh S V, Kumar GM, Balreddy MS, Swamy BC (2011) Liquefaction potential of Sabarmati River sand. *ISET Journal of Earthquake Technology*, Paper No 516:61–71
- Dyvik R, Berre T, Lacasse S, Raadim B (1987) Comparison of truly undrained and constant volume direct simple shear tests. *Geotechnique* 37:3–10
- Ecemis N, Karaman M (2014) Influence of non-/low plastic fines on cone penetration and liquefaction resistance. *Eng Geol* 181:48–57. <https://doi.org/10.1016/j.enggeo.2014.08.012>
- Ecemis N, Monkul MM, Orucu M (2024) Applicability of soil-type index for shear wave velocity-based liquefaction assessment. *Earthq Eng Struct Dyn*. <https://doi.org/10.1002/eqe.4102>
- Erten D, Maher MH (1995) Cyclic undrained behavior of silty sand. *Soil Dyn Earthq Eng* 14:115–123. [https://doi.org/10.1016/0267-7261\(94\)00035-F](https://doi.org/10.1016/0267-7261(94)00035-F)
- Eseller-Bayat EE, Monkul MM, Akin Ö, Yenigun S (2019) The coupled influence of relative density, CSR, plasticity and content of fines on cyclic liquefaction resistance of sands. *J Earthq Eng* 23:909–929. <https://doi.org/10.1080/13632469.2017.1342297>
- Finn WDL, Vaid YP (1977) Liquefaction potential from drained constant volume cyclic simple shear tests. In: *Proceedings of the sixth world conference on earthquake engineering*, pp 2157–2162
- Ghali M, Chekired M, Karray M (2019) A laboratory-based study correlating cone penetration test resistance to the physical parameters of uncemented sand mixtures and granular soils. *Eng Geol* 255:11–25. <https://doi.org/10.1016/j.enggeo.2019.04.015>
- Goudarzy M, König D, Schanz T (2016a) Small strain stiffness of granular materials containing fines. *Soils Found* 56:756–764. <https://doi.org/10.1016/j.sandf.2016.08.002>
- Goudarzy M, Rahman MM, König D, Schanz T (2016b) Influence of non-plastic fines content on maximum shear modulus of granular materials. *Soils Found* 56:973–983. <https://doi.org/10.1016/j.sandf.2016.11.003>
- Goudarzy M, König D, Schanz T (2018) Small and intermediate strain properties of sands containing fines. *Soil Dyn Earthq Eng* 110:110–120. <https://doi.org/10.1016/j.soildyn.2018.02.020>
- Goudarzy M, Sarkar D, Lieske W, Wichtmann T (2022) Influence of plastic fines content on the liquefaction susceptibility of sands: monotonic loading. *Acta Geotech* 17:1719–1737. <https://doi.org/10.1007/s11440-021-01283-w>
- Goudarzy M, Rahemi N, Rahman MdM, Schanz T (2017) Predicting the maximum shear modulus of sands containing nonplastic fines. *J Geotech Geoenviron Eng* 143. [https://doi.org/10.1061/\(asce\)gt.1943-5606.0001760](https://doi.org/10.1061/(asce)gt.1943-5606.0001760)
- Green RA, Terri GA (2005) Number of equivalent cycles concept for liquefaction evaluations-revisited. *J Geotech Geoenviron Eng* 131:477–488. [https://doi.org/10.1061/\(ASCE\)1090-02412005131:4477](https://doi.org/10.1061/(ASCE)1090-02412005131:4477)
- Hazirbaba K, Rathje EM (2009) Pore pressure generation of silty sands due to induced cyclic shear strains. *J Geotech Geoenviron Eng* 135:1892–1905. [https://doi.org/10.1061/\(ASCE\)GT.1943-5606.0000147](https://doi.org/10.1061/(ASCE)GT.1943-5606.0000147)
- Idriss IM, Boulanger RW (2008) *Soil liquefaction during earthquakes*, EERI Monograph No: 12
- Jamiolkowski M, LoPresti DCF, Manassero M (2001) Evaluation of relative density and shear strength of sands from cone penetration test and flat dilatometer test. *Soil Behav Soft Ground Construction GSP* 119:201–238
- Jradi L, Dupla JC, Seif El Dine B, Canou J (2020) Effect of fine particles on cyclic liquefaction resistance of sands. *Int J Geotech Eng* 14:860–875. <https://doi.org/10.1080/19386362.2020.1711555>
- Karim ME, Alam MJ (2014) Effect of non-plastic silt content on the liquefaction behavior of sand-silt mixture. *Soil Dyn Earthq Eng* 65:142–150. <https://doi.org/10.1016/j.soildyn.2014.06.010>

- Khodkari N, Hamidian P, Khodkari H et al (2024) Predicting the small strain shear modulus of sands and sand-fines binary mixtures using machine learning algorithms. *Transp Geotech* 44:101172. <https://doi.org/10.1016/j.trgeo.2023.101172>
- Kokusho T (2007) Chapter 8: liquefaction strengths of poorly-graded and well-graded granular soils investigated by lab tests. *Geotech Geol Earthq Eng* 6:159–184. [https://doi.org/10.1007/978-1-4020-5893-6\\_8](https://doi.org/10.1007/978-1-4020-5893-6_8)
- Kolapalli R, Rahman MM, Karim MR, Nguyen HBK (2023) The failure modes of granular material in undrained cyclic loading: a critical state approach using DEM. *Acta Geotech* 18:2945–2970. <https://doi.org/10.1007/s11440-022-01761-9>
- Kramer SL (1996) *Geotechnical Earthquake Engineering*
- Kwa K, Airey D (2017) Effects of fines on the cyclic liquefaction behaviour in well-graded materials. *Can Geotech J* 54:1460–1471. <https://doi.org/10.1016/j.sandf.2019.03.001>
- Lade PV, Yamamuro JA, Liggio CD Jr (2009) Effects of fines content on void ratio, compressibility, and static liquefaction of silty sand. *Geomech Eng* 1:1–15. <https://doi.org/10.12989/gae.2009.1.1.001>
- Lade PV, Liggio CD Jr, Yamamuro JA, (1998) Effects of non-plastic fines on minimum and maximum void ratios of sand. *Geotech Test J* 21:336–347
- Lade P, Yamamuro J (1997) Effects of nonplastic fines on static liquefaction of sands. *Can Geotech J* 34:918–928. <https://doi.org/10.1139/t97-052>
- Lade PV, Yamamuro JA (2011) Evaluation of static liquefaction potential of silty sand slopes. *Can Geotech J* 48:247–264. <https://doi.org/10.1139/T10-063>
- Lasley SJ, Green RA, Rodriguez-Marek A (2017) Number of equivalent stress cycles for liquefaction evaluations in active tectonic and stable continental regimes. *J Geotech Geoenviron Eng* 143. [https://doi.org/10.1061/\(asce\)gt.1943-5606.0001629](https://doi.org/10.1061/(asce)gt.1943-5606.0001629)
- Li Y, Yang Y, Yu H, Roberts G (2016) Monotonic direct simple shear tests on sand under multidirectional loading. *Int J Geomech* 17:1–10. [https://doi.org/10.1061/\(ASCE\)GM.1943-5622.0000673](https://doi.org/10.1061/(ASCE)GM.1943-5622.0000673)
- Liu A, Stewart JP, Abrahamson NA, Moriwaki Y (2001) Equivalent number of uniform stress cycles for soil liquefaction analysis. *J Geotech Geoenviron Eng* 127:1017–1026
- Lunne T, Robertson PK, Powell JJM (1997) *Cone penetration testing in geotechnical practice*. CRC Press, 352 pages, ISBN-13 : 978-0419237501
- Manmatharajan V, Sivathayalan S (2011) Effect of overconsolidation on cyclic resistance correction factors  $K_\sigma$  and  $K_\alpha$ . In: *Proceeding of the 14th Pan-American conference on soil mechanics and geotechnical engineering and the 64th Canadian Geotechnical Conference*, p 10
- Maurer BW, Green RA, Cubrinovski M, Bradley BA (2015) Fines-content effects on liquefaction hazard evaluation for infrastructure in Christchurch, New Zealand. *Soil Dyn Earthq Eng* 76:58–68. <https://doi.org/10.1016/j.soildyn.2014.10.028>
- Mayne PW (2007) *Cone penetration testing state-of-practice*. NCHRP Project Report Topic 37–1:1–137
- Meyerhof GG (1957) Discussion on research on determining the density of sands by spoon penetration testing. In: *Fourth international conference on soil mechanics and foundation engineering*, pp 3, 110
- Monkul MM, Ozden G (2007) Compressional behavior of clayey sand and transition fines content. *Eng Geol* 89:195–205. <https://doi.org/10.1016/j.enggeo.2006.10.001>
- Monkul MM, Yamamuro JA (2010) Influence of densification method on some aspects of undrained silty sand behavior. In: *Fifth international conference on recent advances in geotechnical earthquake engineering and soil dynamics*. San Diego, p Paper No 1.23a, 1–8
- Monkul MM, Yamamuro JA (2011) Influence of silt size and content on liquefaction behavior of sands. *Can Geotech J* 48:931–942. <https://doi.org/10.1139/t11-001>
- Monkul MM, Gültekin C, Gülver M et al (2015) Estimation of liquefaction potential from dry and saturated sandy soils under drained constant volume cyclic simple shear loading. *Soil Dyn Earthq Eng* 75:27–36. <https://doi.org/10.1016/j.soildyn.2015.03.019>
- Monkul MM, Etminkan E, Şenol A (2016) Influence of coefficient of uniformity and base sand gradation on static liquefaction of loose sands with silt. *Soil Dyn Earthq Eng* 89:185–197. <https://doi.org/10.1016/j.soildyn.2017.06.023>
- Monkul MM, Etminkan E, Şenol A (2017) Coupled influence of content, gradation and shape characteristics of silts on static liquefaction of loose silty sands. *Soil Dyn Earthq Eng*. <https://doi.org/10.1016/j.soildyn.2017.06.023>
- Monkul MM, Yenigün Ş, Eseller-Bayat E (2018) Importance of automatization on dry funnel deposited specimens for liquefaction testing. In: *Geotechnical Special Publication No 293; Slope Stability and Landslides, Laboratory Testing, and In Situ Testing*, ASCE, pp 286–295
- Monkul MM, Kendir SB, Tütüncü YE (2021) Combined effect of fines content and uniformity coefficient on cyclic liquefaction resistance of silty sands. *Soil Dyn Earthq Eng* 151:106999. <https://doi.org/10.1016/j.soildyn.2021.106999>



- Monkul MM, Yenigun S (2021) Automatic funnel control device, US Patent Application No: 17/059,502 ; Publication No: US 2021/0208040 A1. US 2021/02
- Moug DM, Price AB, Parra Bastidas AM et al (2019) Mechanistic development of CPT-based cyclic strength correlations for clean sand. *J Geotech Geoenviron Eng* 145:04019072. [https://doi.org/10.1061/\(asce\)gt.1943-5606.0002101](https://doi.org/10.1061/(asce)gt.1943-5606.0002101)
- Nong ZZ, Park SS, Lee DE (2021) Comparison of sand liquefaction in cyclic triaxial and simple shear tests. *Soils Found* 61:1071–1085. <https://doi.org/10.1016/j.sandf.2021.05.002>
- Oka LG, Dewoolkar M, Olson SM (2018) Comparing laboratory-based liquefaction resistance of a sand with non-plastic fines with shear wave velocity-based field case histories. *Soil Dyn Earthq Eng* 113:162–173. <https://doi.org/10.1016/j.soildyn.2018.05.028>
- Okamura M, Ishihara M, Oshita T (2003) Liquefaction resistance of sand deposit improved with sand compaction piles. *Soils Found* 43:175–187
- Ozener P, Monkul MM, Eseller Bayat E, Ari A, Cetin KO (2024) Liquefaction and performance of foundation systems in Iskenderun during 2023 Kahramanmaraş-Türkiye earthquake sequence. *Soil Dyn Earthq Eng* 178:108433. <https://doi.org/10.1016/j.soildyn.2023.108433>
- Papadopoulou A, Tika T (2008) The effect of fines on critical state and liquefaction resistance characteristics of non-plastic silty sands. *Soils Found* 48:713–725. <https://doi.org/10.3208/sandf.47.887>
- Papadopoulou A, Tika T (2016) The effect of fines plasticity on monotonic undrained shear strength and liquefaction resistance of sands. *Soil Dyn Earthq Eng* 88:191–206. <https://doi.org/10.1016/j.soildyn.2016.04.015>
- Papadopoulou AI, Tika TM (2021) Laboratory-based correlation between liquefaction resistance and shear wave velocity of sand with fines. *Geotechnics* 1:219–242. <https://doi.org/10.3390/geotechnics1020012>
- Park S-S, Kim Y-S (2013) Liquefaction resistance of sands containing plastic fines with different plasticity. *J Geotech Geoenviron Eng* 139:825–830. [https://doi.org/10.1061/\(ASCE\)GT.1943-5606.0000806](https://doi.org/10.1061/(ASCE)GT.1943-5606.0000806)
- Payan M, Senetakis K (2019) Effect of Anisotropic Stress State on Elastic Shear Stiffness of Sand-Silt Mixture. *Geotech Geol Eng* 37:2237–2244. <https://doi.org/10.1007/s10706-018-0690-9>
- Payan M, Khoshghalb A, Senetakis K, Khalili N (2016) Small-strain stiffness of sand subjected to stress anisotropy. *Soil Dyn Earthq Eng* 88:143–151. <https://doi.org/10.1016/j.soildyn.2016.06.004>
- Payan M, Senetakis K, Khoshghalb A, Khalili N (2017) Characterization of the small-strain dynamic behaviour of silty sands; contribution of silica non-plastic fines content. *Soil Dyn Earthq Eng* 102:232–240. <https://doi.org/10.1016/j.soildyn.2017.08.008>
- Payan M, Chenari RJ (2019) Small strain shear modulus of anisotropically loaded sands. *Soil Dyn Earthq Eng* 125. <https://doi.org/10.1016/j.soildyn.2019.105726>
- Polito CP, Martin RJ (2001) Effects of nonplastic fines on the liquefaction resistance of sands. *J Geotech Geoenviron Eng* 127:408–415
- Polito CP (2017) Constant-volume cyclic testing to determine input parameters for the GMP pore pressure generation model. In: *Geotechnical Frontiers 2017: Seismic Performance and Liquefaction (GSP 281)*, ASCE, pp 71–79
- Porcino DD, Diano V (2017) The influence of non-plastic fines on pore water pressure generation and undrained shear strength of sand-silt mixtures. *Soil Dyn Earthq Eng* 101:311–321. <https://doi.org/10.1016/j.soildyn.2017.07.015>
- Porcino D, Caridi G, Ghionna VN (2008) Undrained monotonic and cyclic simple shear behaviour of carbonate sand. *Géotechnique* 58:635–644. <https://doi.org/10.1680/geot.2007.00036>
- Porcino DD, Triantafyllidis T, Wichtmann T, Tomasello G (2021) Application of critical state approach to liquefaction resistance of sand-silt mixtures under cyclic simple shear loading. *J Geotech Geoenviron Eng* 147:04020177. [https://doi.org/10.1061/\(asce\)gt.1943-5606.0002470](https://doi.org/10.1061/(asce)gt.1943-5606.0002470)
- Rahman MM, Lo SR, Gnanendran CT (2008) On equivalent granular void ratio and steady state behaviour of loose sand with fines. *Can Geotech J* 45:1439–1456. <https://doi.org/10.1139/T08-064>
- Rahman MM, Cubrinovski M, Lo SR (2012) Initial shear modulus of sandy soils and equivalent granular void ratio. *Geomech Geoeng* 7:219–226. <https://doi.org/10.1080/17486025.2011.616935>
- Rouholamin M, Bhattacharya S, Orense RP (2017) Effect of initial relative density on the post-liquefaction behaviour of sand. *Soil Dyn Earthq Eng* 97:25–36. <https://doi.org/10.1016/j.soildyn.2017.02.007>
- Salgado R, Bandini P, Member S, Karim A (2000) Shear strength and stiffness of silty sand. *J Geotech Geoenviron Eng* 126:451–462. [https://doi.org/10.1061/\(ASCE\)1090-0241\(2000\)126:5\(451\)](https://doi.org/10.1061/(ASCE)1090-0241(2000)126:5(451))
- Sarkar D, König D, Goudarzy M (2019) The influence of particle characteristics on the index void ratios in granular materials. *Particuology* 46:1–13. <https://doi.org/10.1016/j.partic.2018.09.010>
- Sarkar D, Goudarzy M, König D, Wichtmann T (2020) Influence of particle shape and size on the threshold fines content and the limit index void ratios of sands containing non-plastic fines. *Soils Found* 60:621–633. <https://doi.org/10.1016/j.sandf.2020.02.006>

- Seed H, Idriss IM, Makdisi F, Banerjee N (1975) Representation of irregular stress time histories by equivalent uniform stress series in liquefaction analysis, Report No EERC 75–29. College of Engineering, University of California, Berkeley, Earthquake Engineering Research Center
- Shen CK, Vrymoed JL, Uyeno CK (1977) The effect of fines on liquefaction of sands. In: Proceedings of the 9th international conference on soil mechanics and foundation engineering, Tokyo, pp 381–385
- Singh S (1996) Liquefaction characteristics of silts. *Geotech Geol Eng* 14:1–19. <https://doi.org/10.1007/BF00431231>
- Skempton AW (1986) Standard penetration test procedures and the effects in sands of overburden pressure, relative density, particle size, ageing and overconsolidation. *Geotechnique* 36(3):425–447
- Stamatopoulos CA (2010) An experimental study of the liquefaction strength of silty sands in terms of the state parameter. *Soil Dyn Earthq Eng* 30:662–678. <https://doi.org/10.1016/j.soildyn.2010.02.008>
- Stewart JP, Chu DB, Seed RB, et al (2001) Chi-Chi Earthquake reconnaissance report\_soil liquefaction. *Earthq Spectra* 17:37–60. <https://doi.org/10.1193/1.1586192>
- Thevanayagam S (1998) Effect of fines and confining stress on undrained shear strength of silty sands. *J Geotech Geoenviron Eng* 124:479–491. [https://doi.org/10.1061/\(ASCE\)1090-0241\(1998\)124:6\(479\)](https://doi.org/10.1061/(ASCE)1090-0241(1998)124:6(479))
- Thevanayagam S, Shenthian T, Mohan S, Liang J (2002) Undrained Fragility of Clean Sands, Silty Sands, and Sandy Silts. *J Geotech Geoenviron Eng* 128:849–859. [https://doi.org/10.1061/\(ASCE\)1090-0241\(2002\)128:10\(849\)](https://doi.org/10.1061/(ASCE)1090-0241(2002)128:10(849))
- Tokimatsu K, Yoshimi Y (1983) Empirical correlation of soil liquefaction based on SPT N value and fines content. *Soils Found* 23:56–74
- Troncoso JH, Verdugo R (1985) Silt content and dynamic behavior of tailing sands. In: Proceedings of the 11th international conference on soil mechanics and foundation engineering, vol 3, pp 1311–1314
- Ulmer KJ, Green RA, Rodriguez-Marek A (2022) Recommended b-value for computing number of equivalent stress cycles and magnitude scaling factors for simplified liquefaction triggering evaluation procedures. *J Geotech Geoenviron Eng* 148. [https://doi.org/10.1061/\(ASCE\)GT.1943-5606.0002926](https://doi.org/10.1061/(ASCE)GT.1943-5606.0002926)
- Vaid YP, Sivathayalan S (1996) Static and cyclic liquefaction potential of Fraser Delta sand in simple shear and triaxial tests. *Can Geotech J* 33:281–289. <https://doi.org/10.1139/t96-007>
- Vaid YP, Sivathayalan S (2000) Fundamental factors affecting liquefaction susceptibility of sands. *Can Geotech J* 37:592–606. <https://doi.org/10.1139/t00-040>
- Vaid YP (1994) Liquefaction of silty sands. In: Ground failures under seismic conditions, Geotechnical Special Publication No 44, ASCE, pp 1–16
- Viana Da Fonseca A, Soares M, Fourie AB (2015) Cyclic DSS tests for the evaluation of stress densification effects in liquefaction assessment. *Soil Dyn Earthq Eng* 75:98–111. <https://doi.org/10.1016/j.soildyn.2015.03.016>
- Wei X, Yang J (2019) Characterizing the effects of fines on the liquefaction resistance of silty sands. *Soils Found* 59:1800–1812. <https://doi.org/10.1016/j.sandf.2019.08.010>
- Whitman RV (1971) Resistance of soil to liquefaction and settlement. *Soils Found* 11:59–68
- Wichtmann T, Triantafyllidis T (2009) Influence of the grain-size distribution curve of quartz sand on the small strain shear modulus  $G_{max}$ . *J Geotech Geoenviron Eng*. <https://doi.org/10.1061/ASCEGT.1943-5606.0000096>
- Wichtmann T, Kimmig I, Steller K et al (2019) Correlations of the liquefaction resistance of sands in spreader dumps of lignite opencast mines with CPT tip resistance and shear wave velocity. *Soil Dyn Earthq Eng* 124:184–196. <https://doi.org/10.1016/j.soildyn.2019.05.002>
- Wijewickreme D, Sriskandakumar S, Byrne P (2005) Cyclic loading response of loose air-pluviated Fraser River sand for validation of numerical models simulating centrifuge tests. *Can Geotech J* 42:550–561. <https://doi.org/10.1139/t04-119>
- Xenaki VC, Athanasopoulos GA (2003) Liquefaction resistance of sand-silt mixtures: an experimental investigation of the effect of fines. *Soil Dyn Earthq Eng* 23:183–194. [https://doi.org/10.1016/S0267-7261\(02\)00210-5](https://doi.org/10.1016/S0267-7261(02)00210-5)
- Yamamuro JA, Covert KM (2001) Monotonic and cyclic liquefaction of very loose sands with high silt content. *J Geotech Geoenviron Eng* 127:314–324
- Yamamuro JA, Wood FM, Lade PV (2008) Effect of depositional method on the microstructure of silty sand. *Can Geotech J* 45:1538–1555. <https://doi.org/10.1139/T08-080>
- Yang J, Liu X (2016) Shear wave velocity and stiffness of sand: the role of non-plastic fines. *Geotechnique* 66:500–514. <https://doi.org/10.1680/jgeot.15.P.205>
- Yoshimi Y, Tokimatsu K, Kaneko O, Makihara Y (1984) Undrained cyclic shear strength of a dense Niigata Sand. *Soils Found* 24:131–145
- Youd TL, Idriss IM, Andrus RD et al (2001) Liquefaction resistance of soils: summary report from the 1996 NCEER and 1998 NCEER / NSF workshops on liquefaction. *J Geotech Geoenviron Eng* 127:817–833. [https://doi.org/10.1061/\(ASCE\)1090-0241\(2001\)127:10\(817\)](https://doi.org/10.1061/(ASCE)1090-0241(2001)127:10(817))

- Zhang B, Muraleetharan KK, Liu C (2016) Liquefaction of unsaturated sands. *Int J Geomech* 16. [https://doi.org/10.1061/\(asce\)gm.1943-5622.0000605](https://doi.org/10.1061/(asce)gm.1943-5622.0000605)
- Zuo L, Baudet BA (2015) Determination of the transitional fines content of sand-non plastic fines mixtures. *Soils Found* 55:213–219. <https://doi.org/10.1016/j.sandf.2014.12.017>

**Publisher's Note** Springer Nature remains neutral with regard to jurisdictional claims in published maps and institutional affiliations.